



## Molecular Crystals and Liquid Crystals

Publication details, including instructions for authors and subscription information:

<http://www.tandfonline.com/loi/gmcl20>

### Surface and Interface Tensions Determined From Isotropic Droplets in Freely Suspended Smectic Films

H. Schüring<sup>a</sup> & R. Stannarius<sup>a</sup>

<sup>a</sup> Inst. für Experimentelle Physik I, Universität Leipzig, Leipzig

Version of record first published: 18 Oct 2010

To cite this article: H. Schüring & R. Stannarius (2004): Surface and Interface Tensions Determined From Isotropic Droplets in Freely Suspended Smectic Films, *Molecular Crystals and Liquid Crystals*, 412:1, 425-433

To link to this article: <http://dx.doi.org/10.1080/15421400490431921>

PLEASE SCROLL DOWN FOR ARTICLE

Full terms and conditions of use: <http://www.tandfonline.com/page/terms-and-conditions>

This article may be used for research, teaching, and private study purposes. Any substantial or systematic reproduction, redistribution, reselling, loan, sub-licensing, systematic supply, or distribution in any form to anyone is expressly forbidden.

The publisher does not give any warranty express or implied or make any representation that the contents will be complete or accurate or up to date. The accuracy of any instructions, formulae, and drug doses should be independently verified with primary sources. The publisher shall not be liable

for any loss, actions, claims, proceedings, demand, or costs or damages whatsoever or howsoever caused arising directly or indirectly in connection with or arising out of the use of this material.

## **SURFACE AND INTERFACE TENSIONS DETERMINED FROM ISOTROPIC DROPLETS IN FREELY SUSPENDED SMECTIC FILMS**

*H. Schüring and R. Stannarius*

*Universität Leipzig, Inst. für Experimentelle Physik I,  
Linnéstrasse 5, D-04103 Leipzig*

*Isotropic droplets in freely suspended smectic films are studied by means of optical microscopy. Droplet shapes are determined with an interference method and described with a model that considers the surface and interface tensions of the smectic, isotropic liquid and gas phase. In uniform film regions, droplets adopt the shape of flat lenses. Deformations of the circular droplet contour are observed for droplets lined up at thickness steps in inhomogeneous films.*

*PACS numbers: 61.30.-v 68.15. + e 87.64.Rr*

### **INTRODUCTION**

Phase transitions in freely suspended smectic films have been extensively studied in the past, e.g. in order to determine the influence of surface-enhanced ordering or decreasing dimensionality. Only few experiments dealt with a phenomenon related to the smectic-nematic or smectic-isotropic transition: droplet nucleation in free standing films [1–4]. Local isotropic droplets can nucleate by two different mechanisms. On the one hand, in some materials as non-eutectic smectic mixtures, liquid crystals containing dopants or polymeric smectics, the phase transition to the isotropic phase can be broadened to a biphasic range in which isotropic and smectic regions coexist. It has been shown e.g. that in free standing films of smectics containing photochromic dopants, local isotropic inclusions can be generated by irradiation with UV light. On the other hand, the inner

The authors are indebted to W. Weissflog, R. Zentel and Ch. Tolksdorf, who synthesized and provided the samples. This work was supported by the DFG within *Sonderforschungsbereich* 294 and STA 452/8-3.

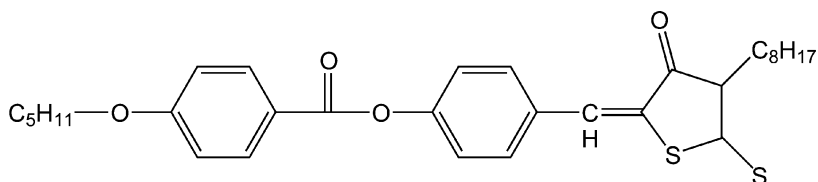
Address correspondence to H. Schüring, Universität Leipzig, Inst. Für Experimentelle Physik I, Linnéstrasse 5, D-04103 Leipzig, Germany.

layers of a smectic film start to melt at temperatures above the bulk phase transition. While at the film surfaces, a smectic region with the thickness of the smectic layer coherence length remains, the liquid material in the center of the film may assemble in droplets in the film plane. This mechanism is an alternative to the well known layer-by-layer thinning transition of free standing smectic films [5]. The formation and stability of droplets is described in detail elsewhere [6]. In the focus of this paper are their equilibrium shapes, which give direct access to interface properties. In particular, very small surface tension differences between smectic and isotropic phases can be determined. Furthermore, arrangement and dynamics of droplets in inhomogeneous films are perfectly suited to study capillary forces mediating long range interactions between single droplets or traction in film thickness gradients. These phenomena are related to capillary forces on colloidal particles, which have been investigated theoretically as well as experimentally previously in liquid films [7]. They are of general interest, for example also in the context of biological membranes [8].

## EXPERIMENTAL

Freely suspended smectic films are drawn across holes of 1–2 mm diameter in a copper or glass substrate, mounted on a METTLER hot stage. For optical observation, an AXIOTECH reflection microscope is used. The samples are illuminated with normal incident white or monochromatic light. A digital CCD camera (Nikon Coolpix 990) is used for image acquisition.

The material used in the surface tension study is the three kernel smectogen PBOT (*3-n-Octyl-5-[4-(4-n-pentyloxybenzoyloxy)benzylidene]-4-oxo-thiazolidin-2-thione*),



with the following phase sequence in the bulk: Cr 106°C SmA 119°C I. The material was chosen because it often forms thick and inhomogeneous films with sharp thickness steps of 100 nm height and more. This allows to observe the deformation of droplets pinned at such thickness steps and forces acting along the droplet boundary can be estimated.

For the observation of droplet nucleation, smectic films are prepared and subsequently heated up with heating rates of about 1 K/min. In

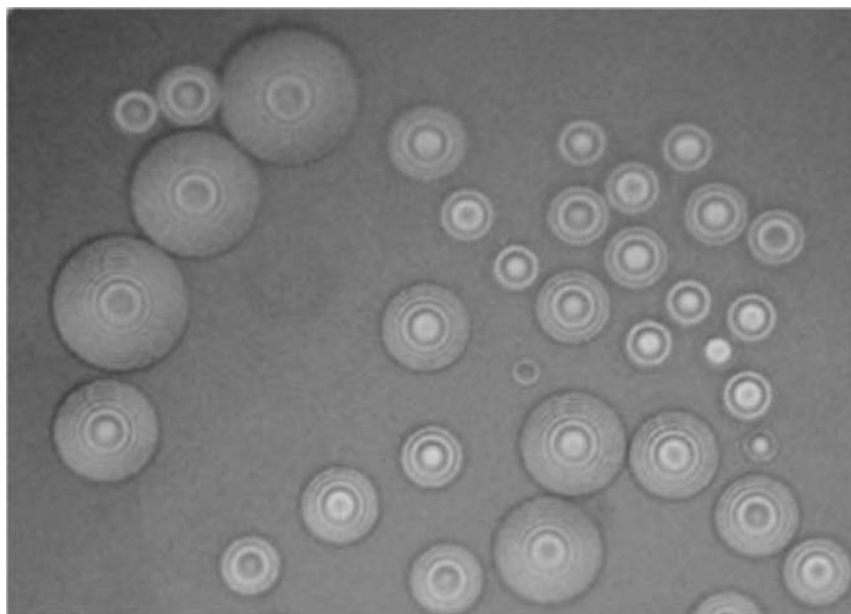


**FIGURE 1** Isotropic droplets of different sizes in a uniform region of a smectic film, observed under monochromatic illumination ( $\lambda = 590$  nm). Image size  $135\ \mu\text{m} \times 100\ \mu\text{m}$ .

contrast to previously observed materials [6], liquid droplets form practically instantaneous over the whole temperature range of the SmA phase. At fixed temperature, a broad distribution of droplet radii in the micrometer range is observed. With increasing temperature, their average size grows. Droplets consist of isotropic material, expelled from internal layers of the film. Therefore, their surface profile is smooth and without the layer steps typically observed in smectic film regions. In monochromatic light, concentric ‘Newton fringes’ are visible which allow the determination of the droplet thickness profile (Fig. 1). In order to evaluate the droplet shape, a suitable model profile (Fig. 2) is chosen and the optical image is simulated with standard methods [9,10]. The droplet radius  $r$  is directly extracted from the reflection image and the maximum droplet elevation  $h$  is the only free parameter in this model to adjust all fringe positions.

## MODEL AND DISCUSSION

The interface tension between smectic and isotropic phase keeps the outer droplet boundary circular, but it is too small to play any role in the droplet

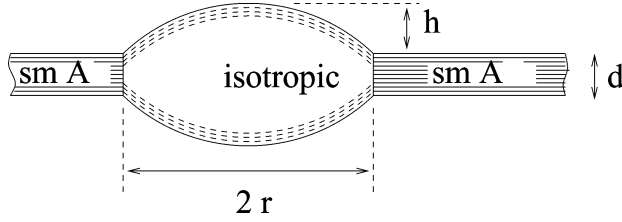


**FIGURE 2** Schematic model of an isotropic droplet in a smectic film. Possible smectic surface layers on the isotropic droplet are indicated by dashed lines. ( $h$  and  $d$  have been exaggerated with respect to  $r$ .)

size and thickness profile. The essential factor is the smectic surface tension to air,  $\sigma_s$ , being somewhat lower than that of the isotropic phase,  $\sigma_I$ . In a film of uniform thickness composed of smectic and isotropic regions, the surface energy could be diminished by compressing the area of liquid regions. However, when the volume of liquid material in a droplet is constant at a given temperature, lateral compression leads to creation of additional film surface. The equilibrium droplet shape results from a balance of the surface tensions of smectic and isotropic material. Our droplet model minimizes the surface energy at constant droplet volume, considering the difference  $\Delta\sigma = \sigma_I - \sigma_s$  between the surface tensions in isotropic and smectic phase. The complete solution of the  $h(r)$  characteristics within a model that allows for an additional interface tension  $\sigma_0^\perp$  at the lateral smectic-isotropic droplet boundary is [6]

$$h(r) = -\frac{\sigma_I}{\Sigma} d' + \sqrt{\left(\frac{\sigma_I}{\Sigma} d'\right)^2 + \frac{\sigma_I - \sigma_s}{\Sigma} r^2 + \frac{\sigma_0^\perp}{2\Sigma} r d'} \quad (1)$$

where  $\Sigma = \sigma_I + \sigma_s - \sigma_0^\perp \frac{d'}{2r}$ , and  $d'$  is the film thickness reduced by an effective thickness of the smectic surface layers.

For droplets with  $r \gg d$ , the slope of the  $h(r)$  curves is

$$\frac{dh}{dr} = \sqrt{\frac{\Delta\sigma}{\sigma_I + \sigma_s}} \quad (2)$$

which allows to extract the surface tension difference  $\Delta\sigma$  from the  $h(r)$  data. The effect of  $\sigma_0^\perp$  is a vertical shift of the curves upwards, the linear slope is independent of  $\sigma_0^\perp$ . In the case of  $\sigma_0^\perp = 0$ , the linear fit of large droplet data intersects the  $h$  axis at  $-d/2$ .

Figure 3 shows the relation between droplet elevation and radius in a PBOT film. The curve represents the analytical solution of  $h(r)$  with  $\sigma_0^\perp = 0$ . The fit gives  $\Delta\sigma/(\sigma_I + \sigma_s) = 0.021$ . Assuming a typical surface

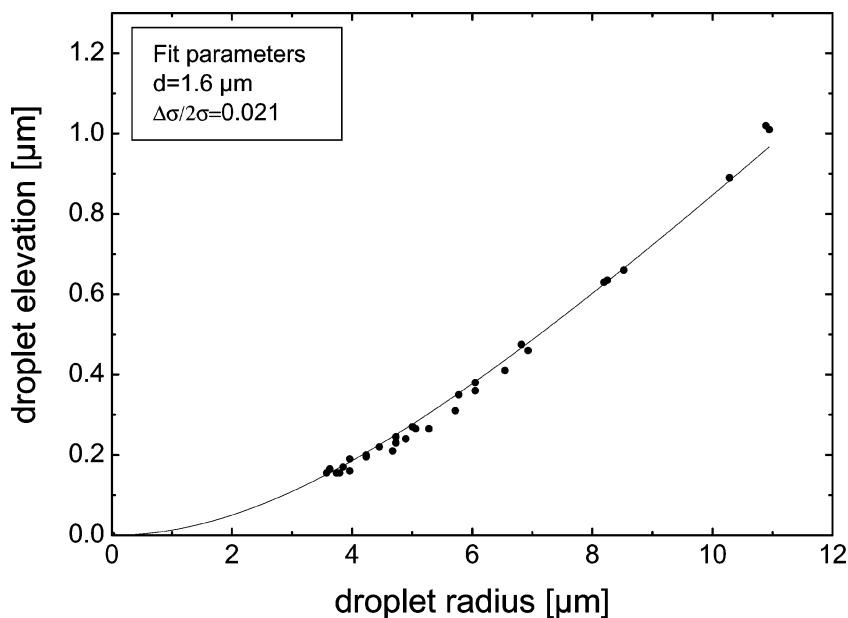


**FIGURE 3** Droplet geometry in PBOT. The fit curve to Eq. (1) has been obtained with  $\sigma_0^\perp = 0$  and  $\Delta\sigma/\sigma_I = 0.042$ ;  $d = 1.6 \mu\text{m}$ .

tension of similar calamitic mesogens of the order of  $0.02 \text{ N/m}$  [11,12], this gives  $\Delta\sigma$  approximately  $840 \mu\text{N/m}$ . At temperatures in the vicinity of the bulk clearing point, a dramatic flattening of the droplets is observed, indicating a tendency of strongly decreasing surface tension difference  $\Delta\sigma$  towards the highest temperature where the smectic film is stable.

## INHOMOGENEOUS FILMS AND CAPILLARY DRAG

Droplets in regions of uniform film thickness do not experience a directed force. However, they are dragged along the film thickness gradient in inhomogeneous regions of the film. When droplets reach a discrete thickness step separating two areas of different film thickness, they are trapped at the edge. At small steps, droplets move almost completely into the thicker region, since they are wetted by the smectic film material. However, at large thickness steps, one can clearly observe that the droplets remain at least partially in the thinner region. The contour of such droplets is found to differ significantly from a circle. A particularly clear deformation is seen in Figure 4.

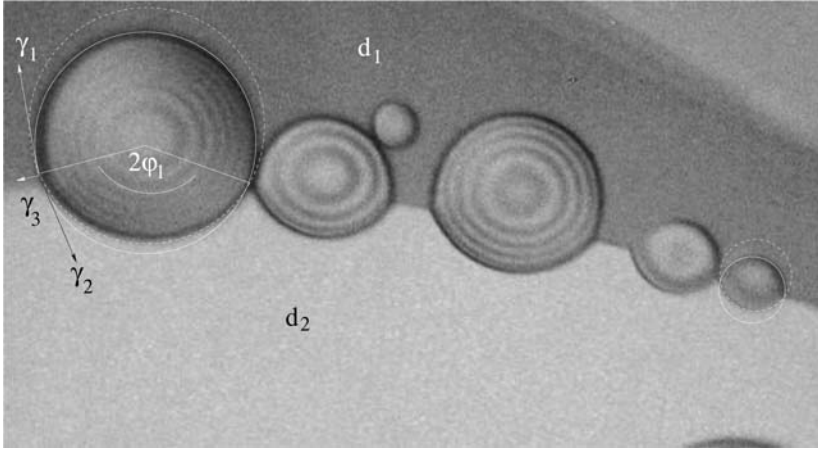


**FIGURE 4** Deformation of droplets lined up at a film thickness step. The 2D projections of all droplets aligned at the step can be described by arcs with radii of curvature  $r_1, r_2$  (indicated for two droplets in the image by circles) in the two regions of different film thickness  $d_1 > d_2$  and by the angle  $\varphi_1$  describing the position relative to the edge. In contrast, cf. the small circular droplet in the uniform film region. The image size is  $180\,\mu\text{m} \times 100\,\mu\text{m}$ .

The thickness step seen in the image is  $\approx 90\,\text{nm}$  ( $d_1 \approx 1690\,\text{nm}$ ). The image allows to construct a force balance condition for the line tensions along the droplet boundary. If the flat droplet is approximated by a disk shape, the problem can be treated in 2D. The energy per length of the 1D projections of the lateral droplet interfaces in the film is represented here by line tensions  $\gamma_i$ . At the intersections of droplet and edge, the forces along the edge direction as well as those perpendicular to it must be balanced in equilibrium. We define  $\gamma_1$  as the line tension of the isotropic-smectic interface in the thick film region,  $\gamma_2$  as the line tension in the thin region, and  $\gamma_{\text{edge}} = \gamma_3$  as the line tension of the thickness step. From

$$\begin{aligned}\gamma_1 \sin \varphi_1 + \gamma_2 \sin \varphi_2 &= 0, \\ \gamma_3 + \gamma_1 \cos \varphi_1 + \gamma_2 \cos \varphi_2 &= 0, \\ r_1 \sin \varphi_1 - r_2 \sin \varphi_2 &= 0,\end{aligned}$$

( $r_1, r_2$  are the radii of curvature of the interfaces in the thick and thin regions, resp., and  $\varphi_1$  is defined in Fig. 4), one obtains the ratios  $\gamma_2/\gamma_1 = r_2/r_1$  and  $\gamma_3/\gamma_1 = ((r_2/r_1)^2 - \sin^2 \varphi_1)^{0.5} - \cos \varphi_1$  in terms of the measurable geometrical quantities  $r_1, r_2$  and  $\varphi_1$ . In the limit of  $\Delta r = r_2 - r_1 \ll r_1$  and small  $\varphi_{1,2}$ , a good approximation of the latter ratio



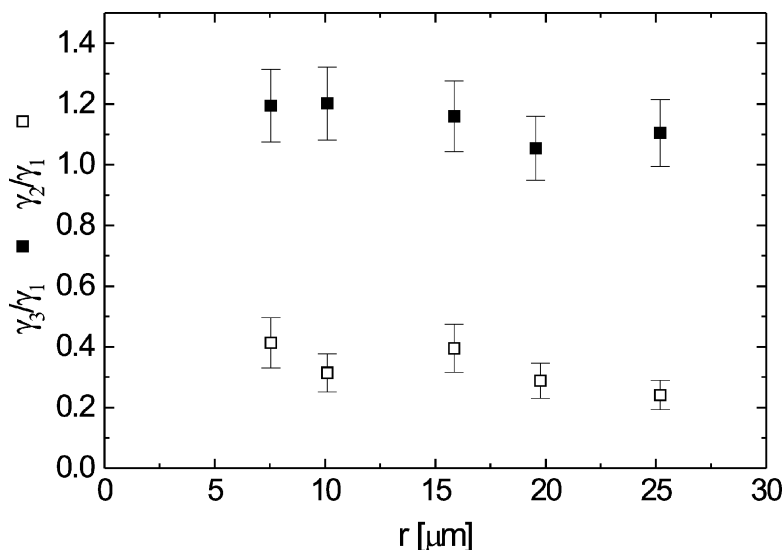


**FIGURE 5** Ratios of the line tensions  $\gamma_3/\gamma_1$  and  $\gamma_2/\gamma_1$  determined from the radii and angles of the droplets in Figure 4.

is  $\gamma_3 \approx \Delta r / (r_1 \cos \varphi_1)$ . Figure 5 shows the results obtained for the five droplets of Figure 4. The average radius ratio is  $r_2/r_1 = 1.09$ , and  $\varphi_1$  decreases from  $\approx 90^\circ$  to about  $70^\circ$  with increasing  $r$ . A slight trend is found to larger values in  $\gamma_3/\gamma_1$  towards smaller droplet sizes. The small droplets are more oblate than the large size ones. This is probably a consequence of the fact that the preconditions of the simple two-dimensional model are better matched for the small bubbles.

If the film thickness step is small, the angles  $\varphi_{1,2}$  are close to zero, indicating that the sum of  $\gamma_1 + \gamma_3$  is only slightly larger than  $\gamma_2$  in most of the observed cases. It has been observed in all smectogens (about half a dozen of chemically different compounds, including e.g. DOBAMBC, have been studied qualitatively) without exception that the droplets are pinned at layer steps, i.e. the principle of the trapping mechanism discussed above can be expected to be general. When droplets are in contact with multiple layer steps, a directed motion along the thickness gradient is observed until they reach a plateau border or the meniscus.

## DISCUSSION AND SUMMARY

It has been shown that isotropic droplets in smectic films can be analysed quantitatively to obtain interface tensions and capillary forces in liquids.

The shapes of these objects can be explained with a model that allows for small surface tension differences between smectic and isotropic phases. As the differences in  $\sigma$  are about two orders of magnitude smaller than the absolute values of  $\sigma_I$  and  $\sigma_S$ , they are not accessible with conventional surface tension measurements. One can understand the excess surface tension contribution in the isotropic phase if one takes into account that the isotropic bulk material is covered by smectic surface layers, and the tension of the additional interface formed between the isotropic regions and the smectic surface layers contributes to  $\sigma_I$ .

The pinning of droplets at layer steps is also explainable at least qualitatively. It is worth noting that at the step, the effective line tension of the droplet in the thicker film,  $\gamma_1$ , is smaller than  $\gamma_2$  in the thinner film. This difference provides the driving force that drags the droplets into thicker film regions. Within a rather crude 2D model (vertical interfaces), one may assign the line tension  $\gamma_1$  to  $d'_1 \sigma_o^\perp$ ,  $\gamma_2 \approx d'_2 \sigma_o^\perp + (d_1 - d_2) \sigma_S^\perp$  and  $\gamma_3 \approx (d_1 - d_2) \sigma_S^\perp$ , where  $d'_1, d'_2$  are the respective film thicknesses corrected for some smectic surface layers, and  $\sigma_S^\perp$  is the surface tension of the smectic phase to air at an interface perpendicular to the layers. This model is consistent with the finding  $\gamma_3 + \gamma_1 \approx \gamma_2$  for many materials when  $d_1 - d_2$  is small (droplets are almost completely immersed in the thick film region). At a large step as in Figure 4,  $\gamma_2$  is noticeably smaller than predicted from the simple 2D assignment, because the isotropic droplet has a more complex, flattened shape on the thin film side (see the additional interference fringe in the lower part of the droplets in Fig. 4). If one compares, within such a simple model, the experimental finding  $\gamma_3 \approx 0.3\gamma_1$  with the assignments for  $\gamma_3$  and  $\gamma_1$ , one finds  $\sigma_S^\perp = 0.3 d'_1 / (d_1 - d_2) \sigma_o^\perp \approx 5.6 \sigma_o^\perp$ . This result should, however, not be overestimated because of the crude simplifications in the model and the large error (in particular when  $d'_1$  is approximated by  $d_1$ ). By means of systematic quantitative studies of the droplet shapes in dependence on the step height, however, the model may certainly be improved and information about the interface properties of isotropic liquid, smectic and gas phases may be achieved.

Summarizing, it has been shown that the study of geometrical properties of isotropic liquid droplets on smectic films may serve as a new tool to access surface and interface tensions of liquid crystalline mesophases.

## REFERENCES

- [1] Cluzeau, P., Dolganov, V. K., Poulin, P., Joly, G., & Nguyen, H. T. (2001). *Mol. Cryst. Liq. Cryst.*, **364**, 381.
- [2] Dolganov, V. K., Demikhov, E. I., Fouret, R., & Gors, C. (1996). *Physics Letters A*, **220**, 242.
- [3] Pankratz, S., Johnson, P. M., Paulson, A., & Huang, C. C. (2000). *Phys. Rev. E*, **61**, 6689.

- [4] Najjar, R. & Galerne, Y. (2001). *Mol. Cryst. Liq. Cryst.*, 367, 475.
- [5] Stoebe, T., Mach, P., & Huang, C. C. (1994). *Phys. Rev. Lett.*, 73, 1384.
- [6] Schüring, H. E. & Stannarius, R. *Langmuir*, (in press).
- [7] Sur, J. & Pak, H. K. (2002). *Phys. Rev. Lett.*, 86, 4326.
- [8] Schiller, P. (2000). *Phys. Rev. E*, 62, 918.
- [9] Kraus, I., Pieranski, P., Demikhov, E. I., Stegemeyer, H., & Goodby, J. (1993). *Phys. Rev. E*, 48, 1916.
- [10] Stannarius, R., Cramer, C., & Schüring, H. E. (1999). *Mol. Cryst. Liq. Cryst.*, 329, 423.
- [11] Mach, P., Huang, C. C., Stoebe, T., Wedell, E. D., Nguyen, H. T., de Jeu, W. H., Guittard, F., Naciri, J., Sashidar, R., Clark, N., Jiang, I. M., Kao, J. F., Liu, H., & Nohira, H. (1998). *Langmuir*, 14, 4330.
- [12] Schüring, H. E., Thieme, C., & Stannarius, R. (2001). *Liq. Cryst.*, 28, 241.